Accuracy of the Liouville mapping across the shock

Early measurements in the vicinity of the Earth's bow shock provided typical structures of the electron distribution function. An extreme behavior is observed in the thin region of the shock magnetic ramp, where the electron (and ion) temperature changes rapidly. Several mechanisms were proposed for describing the apparent acceleration of the electron beams in this region. Among them, recent studies based on Cluster data have shown that the electron energization and temperature increase can be explained in terms of guiding center motion in the smooth electric and magnetic fields inside the shock ramp. In order to check this mechanism, we applied the Vlasov–Liouville mapping, following the electron distribution function between the upstream and downstream boundaries of a simulated supercritical fast mode shock. The 1-D full particle simulation code was run for roughly 10 ion gyroperiods, with the following parameters: incident angle $\theta_{Bn} = 80°$, Alfvén Mach number of the injected solar wind plasma $M_A = 8$, ion to electron mass ratio $m_i/m_e = 500$, squared ratio of the electron plasma frequency to gyrofrequency $(\omega_{pe}/\Omega_{ce})^2 \equiv \tau = 64$, plasma $\beta = 0.1$ for both electrons and ions. The simulation procedure was adjusted in order to define and follow collections of particles that are transmitted, reflected, or trapped at the shock ramp. The Vlasov–Liouville mapping was performed from the upstream region to a thin surface from the foot of the shock. The results demonstrate a similar behavior for the source and the mapped distribution functions, except for some unpredicted structures, located at higher electron energies. Further mappings to the overshoot and downstream regions may clarify this aspect, and help to understand the limits of the adiabatic approach in the investigation of the electron energization at quasi-perpendicular collisionless shocks. The results obtained by simulations could also be compared with recent studies based on the analysis of Cluster data.

In the simulation above, an important limitation in constructing accurate distribution functions was the low statistics due to reduced particle density. The typical values used in PIC simulations are not large enough to compute the distribution functions for a broad pitch-angle range at different energies. The increase in the particle density is limited by hardware and software constraints. One has to modify the PIC code to work in a 64-bit Unix environment, in order to improve the memory access. Another important constraint is the time needed for a given simulation run. The higher is the input particle density, the longer is the simulation run time and optimizations are needed among the input parameters.

The distribution functions are computed in different regions relative to the ramp of the shock. The upstream distribution functions are then transported to downstream positions via Liouville mapping and compared with the distributions provided by the PIC code (see Figure 1). One can also apply a second, approximate Liouville mapping, assuming that the magnetic moment and energy are conserved along particle trajectories in the de Hoffmann-Teller frame (referred here as adiabatic Liouville mapping).

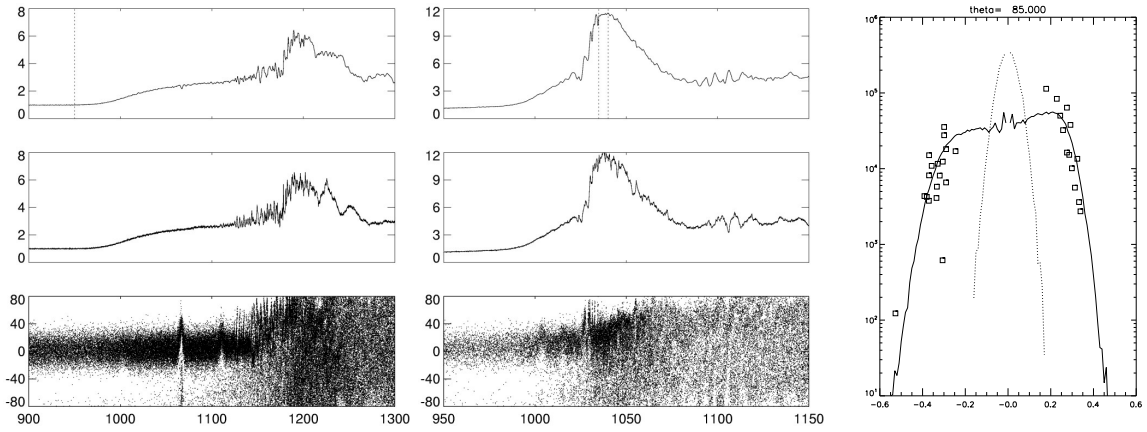

Figure 1: *Left and center:* Profiles of the B_z/B_0 component of the magnetic field, n_e/n_0 electron densities, and v_{xe} electron velocity phase space, at $t\Omega_{ci}$=3.57 (initial) and $t\Omega_{ci}$=4.53 (final). B_z and n_e are normalized to the upstream values while v_{xe} is given in units of upstream Alfvén wave speed, v_A. The location, *x*, along the simulation box is measured in electron inertial lengths, λ_e. *Right:* Electron distribution functions in the plasma system at θ=85^o pitch angle. The PIC distributions from far upstream, left of x=950λ_e, and from the overshoot region, x=1025-1030 λ_e (see the vertical dashed lines in the magnetic field profiles), are plotted by dashed and solid line, respectively, while the Liouville mapped values are indicated by small squares.

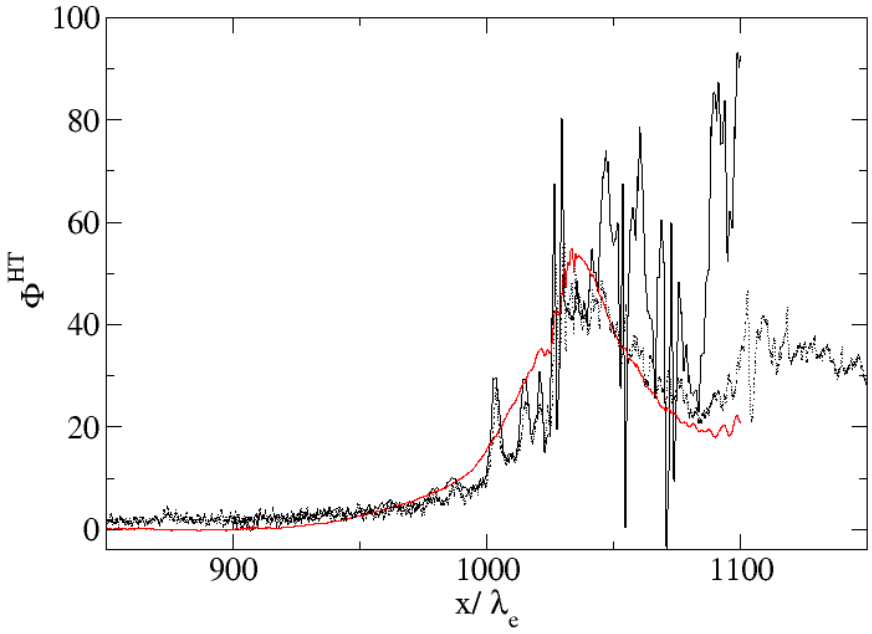

Figure 2: Cross-shock potential as obtained by three different approaches: by fitting the Liouville mapped distribution function to the actual one (black solid); by direct integration of the electric field obtained from the PIC simulation (red); by polytrope approximation of the fluid theory, $\gamma/(\gamma-1)[KT_e]$ (black dotted).

The cross shock potential obtained by the PIC code is compared to the one obtained from the adiabatic Liouville mapping in Figure 2 (*Comişel and Scholer, 2011*). The adiabatic Liouville mapping estimation follows the trend of the PIC potential, but the differences are at times significant, in particular behind the overshoot of the shock. These differences are probably related to several competing factors. Among them, the large forbidden regions in the velocity space of the upstream incoming electrons, the strong non-stationarity of the shock, and the difficulty to define a proper de Hoffmann-Teller frame in the shock layer.